IMPROVEMENT OF ELECTRIC CHARGING EFFICIENCY OF THE FILTRATION MEDIA

Marius - Cristian PLOPEANU[1], Laurențiu – Marius DUMITRAN[2], Petru V. NOȚINGHER[3], Mirela VIHACENCU[4], Lucian DĂSCĂLESCU[5]

One of the electrode configuration mostly-used for the electrostatic charging of filtration media is the dual wire-cylinder electrode. If the charged zones are not well controlled, electric discharges may occur and endanger the equipments (electric or electronic) near the electrode.

This paper presents the numerical calculation of the electric field and space charge density generated by a dual wire-cylinder electrode to which a limiting metallic cylinder was attached. The role of this additional electrode is to reduce the area on which the charge generated by the ionizing wire is collected at the surface of the grounded electrode and hence to increase the charge density in the active zone of the device. The numerical results confirm the fact that the charge is confined to a smaller volume and its density is higher when attaching this cylinder to the standard dual electrode. A simple experiment validated the theoretical predictions and the numerical simulations.

Keywords: filtration media, corona discharge, corona electrodes, electric field, space charge

1. Introduction

A filter medium is a porous and spongy material which allows a fluid (gas or liquid) to pass through and it retains impurities (solid particles) found in suspension in that fluid [1, 2]. Such media can be encountered in water purification, biotechnologies, chemical and pharmaceutical industries, minerals beneficiation [1]. The filters are made of different types of fibers: synthetic (polypropylene, polyethylene, polyester, polystyrene, etc.) or natural (cotton, wool, etc.) [1].

[1] PhD Student, Faculty of Electrical Engineering, University POLITEHNICA of Bucharest, Romania, e-mail: marius.plopeanu@hotmail.com

[2] Assoc. Prof., Faculty of Electrical Engineering, University POLITEHNICA of Bucharest, Romania.

[3] Prof., Faculty of Electrical Engineering, University POLITEHNICA of Bucharest, Romania

[4] PhD Student, Faculty of Electrical Engineering, University POLITEHNICA of Bucharest, Romania

[5] Prof., PPRIME Institute, CNRS – University of Poitiers – ENSMA, IUT d'Angoulême. Electrostatics and Dual – Phase Flow Research Unit

The fibers composing such media can be either woven or non-woven. Two technologies are commonly considered for the fabrication of non-woven media: needle punching (pressing the fibers using two plates, one of which is provided with metal needles), and melt-blowing (blowing the fibers with very hot air and pressing them using a drum system) [1].

The media made of pressed polymeric fibers have recently gained a substantial place on the market. The filtering proprieties of these media are improved when they are electrically charged (Fig. 1). An optimal balance is achieved between filtration efficiency and pressure loss during service [2-7].

The filtration efficiency η_f is defined by the relation [1]:

$$\eta_f = \left(1 - \frac{N_{av}}{N_{am}}\right) \cdot 100 \ [\%] \tag{1}$$

where N_{av} represents the number of downstream particles and N_{am} the number of upstream particles.

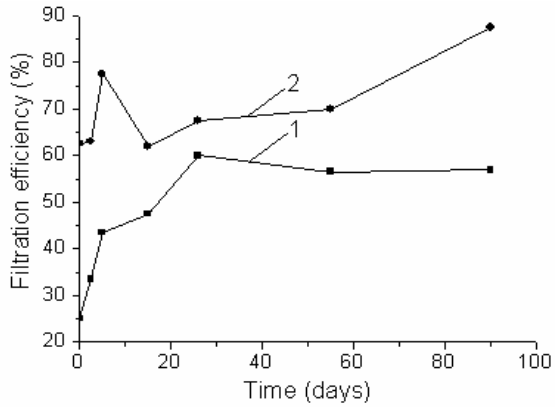

Fig. 1. Variation of the filtration efficiency with usage time for an (1) uncharged and electric charged (2) filter media [4].

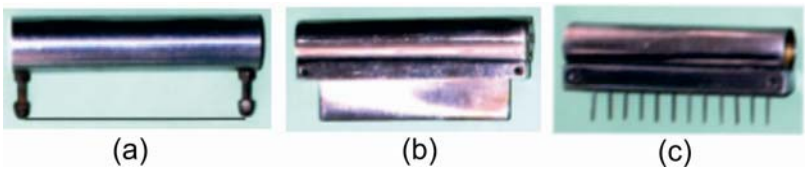

Fig. 2. Different electrode configurations used for electrical charging of insulating (dielectric) materials: a – needles-type electrode; b – blade-type electrode; c – dual wire-cylinder electrode [7].

Currently, the electric charging of filtration media is performed using corona discharges obtained with different types of electrode arrangements (Fig. 2), such as dual wire-cylinder electrode, blade-cylinder electrode, needles-cylinder electrode, needle [8-9]. Although it is more exposed to mechanical damage than the blade – type or needle type electrodes [10], the dual wire-cylinder electrode is the device most commonly used for the electrostatic charging of the dielectric materials [10-11].

Corona discharge is a self-sustaining discharge that occurs when there is a potential difference between two asymmetric electrodes (such as a very thin metallic wire or a metal tip and a cylinder or a metal plate connected to the ground) [12-16]. Due to the high intensity of the electric field near the electrode characterized by a small diameter (wire or metal needle), a small zone of air around the wire gets ionized [12], [14], [16]. The resulting ions are directed towards the grounded electrode (metallic grounded plate electrode), so that the material disposed on its surface is subjected to electric charging.

One of the problems that can occur during the charging of filtration media in the manufacturing process is a uniform flux of ions in order to obtain a constant charge density at the surface and within the media. Also, there may be some situations of practical interest requiring the discharge zone to be designed so that to limit the spatial dispersion of the electric charges produced by the corona effect to other elements that are located in the close vicinity of the emitting electrode.

Such a design was presented by Rafiroiu et al. [10] where the dual wire-cylinder electrode was employed together with a bigger, tubular, non-ionizing electrode attached next to it. For the dual wire-cylinder electrode and a plate-type grounded electrode, Caron and Dascalescu [17] proposed a solution for the numerical analysis of the electric field E in the presence of space charge characterized by the volume density ρ. The results provide a very precise picture of the variation of electric field and space charge density at the surface of the grounded electrode. The numerical model was validated by comparing the computed and experimental current-voltage characteristics.

Also, for the dual wire-cylinder electrode facing a plate - type grounded electrode, Dumitran et al. [18-19] proposed a numerical method to calculate the electric field and space charge density based on the conformal transformation. The accuracy of this method has been validated by comparing the computed and experimental current-voltage characteristics and current density distributions at the surface of the grounded electrode.

The aim of this paper is to compute the variation of electric field and volume space charge density in the case of a dual wire – cylinder electrode system with an additional metallic cylinder attached next to it (Fig. 3).

2. Calculation model

2.1. Hypotheses

The dual wire-cylinder electrode consists of a metallic cylindrical electrode (1) (diameter: D_{cyl} = 25 mm) and a very thin wolfram wire (2) (diameter: g_w = 0.07 mm) (Fig. 3). A metallic cylindrical electrode of smaller diameter d_{cyl} = 13 mm, called "limiting cylinder", is placed in the close vicinity of the wire and parallel to it (Fig. 3).

For the calculation of the electric field the following simplifying hypotheses were adopted [18], [20]:

- the ionization zone around the wire is a monopolar charge generator;
- the region between the wire and the plate-type electrode (4) is characterized by a flow of the monopolar ions, from wire to plate;
- the medium is air with the permittivity ε_0.

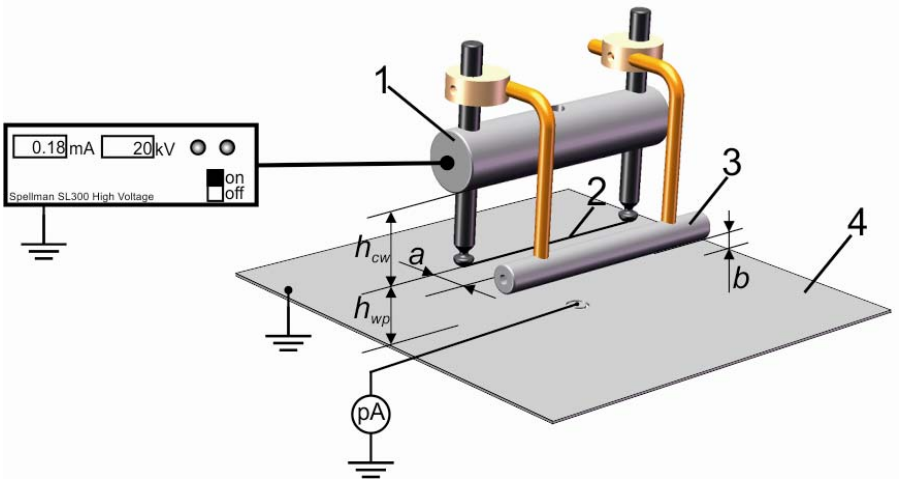

Fig. 3. Schematic representation of the experimental set-up.

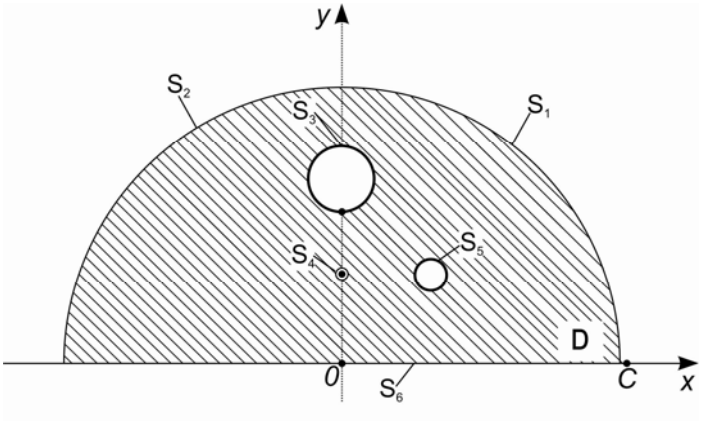

Fig. 4. The schematic representation of the calculation domain.

2.2. Equations

Numerical calculations demand solving the Poisson's equation, the electric potential theorem and the electric charge conservation law [19], [21-22]:

$$\begin{cases} \Delta V = -\dfrac{\rho}{\varepsilon_0} \\ \vec{E} = -gradV \\ div\left(\rho \cdot \mu \cdot \vec{E}\right) = 0 \end{cases} \tag{1}$$

where V is the electric potential, E – the electric field, ρ is the space charge volume density and $\mu = 2 \cdot 10^{-4}$ m^2/V·s - the mobility of the electric charge carriers [18].

2.3. Calculation domain

It is considered that the electric field is plan-parallel (the lines of the electric field are situated in *x0y* plan, perpendicular to the axis of the emitting wire, *Oz* axis) therefore reducing the problem to a bidimensional one. The computations were done in the two quadrants of the Cartesian coordinates system, respectively - $\infty < x < +\infty$ and $0 \le y < +\infty$.

The limits of the finite calculation domain D (Fig. 4) are the curves S_1 and S_2, similar to field lines (which are far enough from the zone of interest for not significantly altering the conclusions of the study), and S_3, S_4, S_5 and S_6 corresponding to the surfaces of the wolfram wire, metallic cylinder, limiting cylinder and grounded electrode, respectively [18], [19], [21].

2.4. Boundary conditions

The conditions imposed to the boundaries of *D* are [16], [18], [20]:
a) For the Poisson equation:

- Dirichlet: $V(M) = V_0,\ M \in S_3 \cup S_4 \cup S_5$;
  $V(M) = 0;\ M \in S_6$;
- Neumann: $\frac{\partial V}{\partial \vec{n}}(M) = 0,\ M \in S_1 \cup S_2$.

where V_0 is the imposed potential at the designated boundary surface.

b) For the electric charge conservation law:

Atten [22] proved that the necessary condition for solving this equation is to impose a constant value of the charge density ρ_0 at the surface of ionizing wire:

$$\rho(M) = \rho_0,\ M \in S_4 .$$

where ρ_0 the space charge density at the surface of the wire.

The value of ρ_0 is chosen so that the numerically-calculated value of ionic current intensity is equal to the one obtained by experiment.

2.5. Non-dimensionalisation

For simplifying the numerical calculations, the quantities *V*, *E* and ρ were replaced with reported associated quantities, respectively with $V^* = \frac{V}{V_{ref}}$, $E^* = \frac{E \cdot h_{wp}}{V_0}$ and $\rho^* = \frac{\rho \cdot h_{wp}^2}{\varepsilon_0 \cdot V_0}$, where V_{ref} is the reference potential which corresponds to the applied potential V_0 mentioned in Dirichlet boundary conditions ($V_{ref} = V_0$), h_{wp} is the distance between the wire and the grounded plate and $\varepsilon_0 = 8.854 \cdot 10^{-12}$ F/m is the vacuum permittivity.

Therefore the equation system (1) becomes [18, 19]:

$$\begin{cases} \Delta^* V^* = -\rho^* \\ \vec{E}^* = -grad^* V^* \\ div^*(\rho^* \cdot \vec{E}^*) = 0 \end{cases} \tag{2}$$

The boundary conditions become [18]:

a) For the Poisson equation:

- Dirichlet: $V^*(M) = 1,\ M \in S_3 \cup S_4 \cup S_5$;

$$V^*(M) = 0,\ M \in S_6;$$

- Neumann: $\frac{\partial V^*}{\partial \vec{n}}(M) = 0,\ M \in S_1 \cup S_2$.

b) For the electric charge conservation law:

$$\rho^*(M) = \rho_0^*,\ M \in S_4.$$

The value of ρ_0^* was chosen in such a way that the computed current at the surface of the grounded plate to be equal to the measured one, respectively $I_m = 27.5$ μA [23].

If $\rho_0^* < 1$, the space charge injected by the wire electrode is too weak for the corona discharge between the wire and the grounded electrode to occur [21]. However, for $\rho_0^* > 1$, a corona discharge is established between the two electrodes [21].

The numerical calculations were performed in Comsol Multiphysics, by the finite elements method (FEM). In order to solve the equation system (2), two PDE (Partial Difference Equation) modules were employed: a module to solve Poisson's equation ("Poisson's Equation") and another for the equation describing charge conservation law ("Coefficient form").

3. Results

The numerical calculations and experimental measurements were carried out for a distance between the wire and the grounded electrode h_{wp} = 45 mm, between the metallic cylinder and the wire h_{cw} = 30 mm, between the limiting cylinder and the grounded electrode b = 45 mm, and two values of the distance between the limiting cylinder and the grounded metallic plate – type electrode, respectively a = 25 and a = 30 mm (Fig. 3). The area A_{probe} of the copper probe (Fig. 3), where the current intensity was measured is 2.5 mm^2. The value of the potential V_0 was 24 kV.

3.1. Numerical results

Figure 5 presents the variation of the non - dimensional electric potential V^* with y-coordinate, in the absence (1) and in the presence (2) of electric space charge, for V_0 = 24 kV.

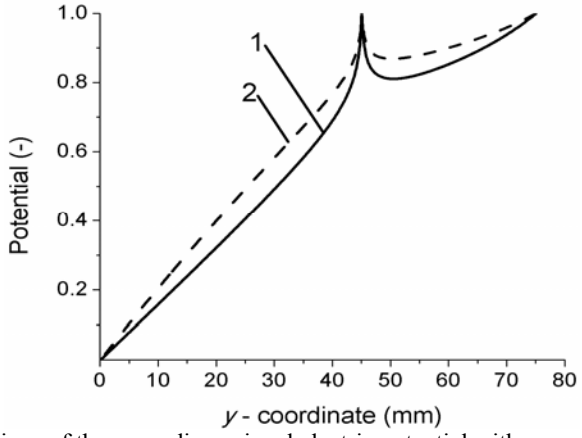

Fig. 5. Variations of the non - dimensional electric potential with *y*-coordinate in the absence (1) and in the presence of electric space charge density (2) (a = 25 mm, V_0 = 24 kV, $\rho_0^* = 8$).

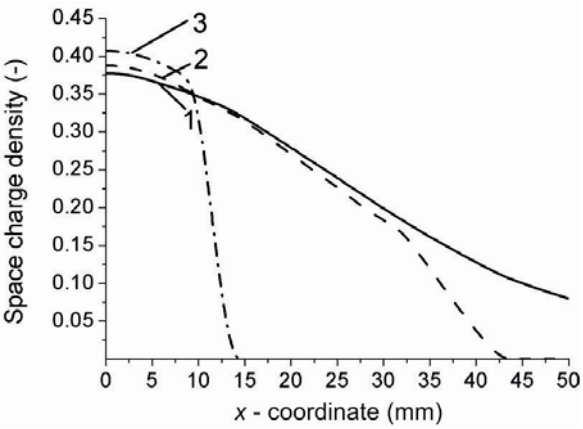

Fig. 6. Variation of the volume space charge density with *x*-coordinate for: 1 – simple wire-plate geometry; 2 – dual wire – cylinder electrode; 3 – dual wire – cylinder electrode with limiting cylinder ($y = 0, V_0$ = 24 kV).

In both cases, the potential increases with *y*-coordinate and that the presence of the electric charge between the tungsten wire and the grounded electrode leads to an increase of the electric potential between the two asymmetric electrodes (the space charge having the same sign (positive) as the potential V_0).

Figure 6 presents the variation of the volume space charge density with *x*-coordinate. For all the electrode configurations, the volume space charge density decreases along the *x*-coordinate.

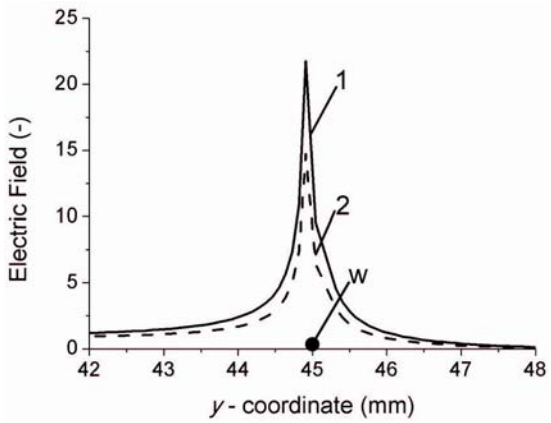

Fig. 7. Variations of the non - dimensional electric field with *y*-coordinate in the absence (1) and in the presence of electric space charge density (2) (a = 25 mm, $\rho_0^* = 8$, w – ionizing wire)

In the case of the wire-plate arrangement (curve 3), the value of the space charge density in the point *O* is the lowest, but the electric charge is distributed along a larger area at the surface of the plate electrode. The presence of the cylinder placed above the wire (curve 2) and of the "limiting cylinder" in the close vicinity of the wire (curve 1) determines an increase of volume space charge density at the surface of the grounded plate for $x < 12.5$ mm. Thus, for the same injection conditions ($\rho_0^* = 8$), the value of space charge density in the *O* point (Fig. 4) is $\rho_{lc}^* = 4.013$ in the case of the dual wire-cylinder electrode with "limiting cylinder" and $\rho_{le}^* = 3.73$ in the case simple dual wire - cylinder arrangement. By consequence, when using the limiting cylinder, the space charge density increases by about 7 %.

For $x > 12.5$ mm, the values of space charge density corresponding to the dual electrode with "limiting" cylinder are lower than those of the wire-plate arrangement and diminish rapidly to zero. Thus, the space charge density decreases by 76 % - for the dual wire - cylinder electrode with "limiting cylinder" - and by 13 % - for the dual electrode wire-cylinder - when x increases from 0 to 12.5 mm .

In Figure 7 the electric field E^* variations with y - coordinate in the absence (curve 1) and in the presence of space charge of volume density $\rho_0^* = 8$ (curve 2) are presented. In the both cases, the values of the electric field are maximum in the vicinity of the wire electrode and that, in the presence of the space charge, for 42 mm < y < 48 mm the electric field values are smaller than in the its absence. This is due to the screen effect of the space charge, which has the same sign as the potential V_0.

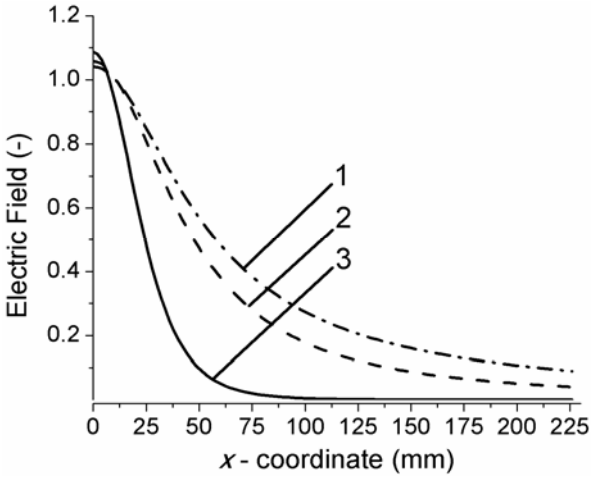

Fig. 8. Variation of the electric field with *x*-coordinate for: 1 – simple wire-plate geometry; 2 – dual wire – cylinder electrode; 3 – dual wire – cylinder electrode with limiting cylinder (V_0 = 24 kV).

For $0 < y < 42$ mm the values of the electric field are higher in the presence than in the absence of the space charge and for 48 mm $< y <$ 75 mm the electric field in absence of space charge is bigger than in the presence of the space charge. It should also be noted that, in the presence of the space charge, there is a point between the wire and the plate-type electrode (for y = 37 mm) in which the electric field is much reduced (E^* = 0.8), then it begins to increase (up to approximately 25 % in the presence of electric charge). Also, between the wire and the cylinder there is a point where the electric field in zero (y = 49 m).

Figure 8 presents the variations of the electric field with x - coordinate, at the surface of the grounded electrode for three configurations of electrodes: wire-plate, dual wire – cylinder electrode and dual wire – cylinder electrode with "limiting cylinder". The applied potential is V_0 = 24 kV. It is noticed that, for all the electrodes arrangements, the electric field decreases along *Ox* axis, from the point *O* to the point *C* situated at the border of the calculation domain (Fig. 4). This is due to the decreasing of space charge density along the *Ox* (Fig. 6).

Decreasing of electric field is more important in the case of dual wire cylinder electrode with "limiting cylinder", than in the case of wire-plate arrangement. Thus, in the case of the dual wire-cylinder electrode with "limiting cylinder" the electric field decreases from the value E_{lc}^* = 1.1 – in the point *O* - to E_{lc}^* = 0.03 in the point of coordinate x = 75 mm, by approximately 97 %.

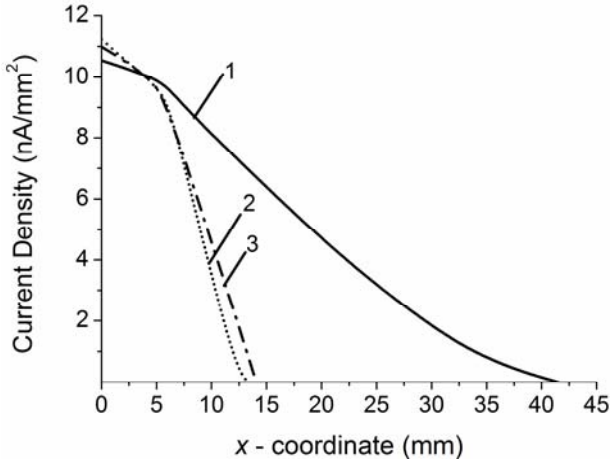

Fig. 9. Variation of the current density with x - coordinate for: 1 - dual wire – cylinder electrode; 2 – dual wire – cylinder electrode with limiting cylinder and a = 25 mm; 3 – dual wire – cylinder electrode with limiting cylinder and a = 30 mm (y = 0, V_0 = 24 kV).

In the case of the simple dual wire - cylinder electrode the electric field decreases by only 74 %, from E_w^* = 1.04 (in O) to E_w^* = 0.27 (in x = 75 mm).

On the other hand, in the vicinity of point O, the electric field is more intense in the case of dual wire – cylinder electrode with limiting cylinder (Fig. 8, curve 3) than in the case of wire – plate arrangement (Fig. 8, curve 1). This is due to the fact that, the space charge density has the highest values in the case of dual wire – cylinder electrode with "limiting cylinder" (Fig. 6, curve 3) and the lowest in the case of in the case of wire-plate arrangement (Fig. 6, curve 1).

3.2. Experimental results

Figure 9 presents the variations of current densities with x – coordinate at the surface of the plate electrode (measured for V_0 = 24 kV) for the dual electrode wire-cylinder (curve 1) and the dual electrode wire- cylinder with limiting cylinder (curves 2 and 3). For the both cases, the courant density decreases rapidly with th x – coordinate. Thus, for a = 25 mm (curve 2), if x increases from 0 to 12.5 mm, the current density J decreases by 94%, from $J_{\max}$ = 11.4 nA/mm^2 to $J_{12.5mm}$ = 0.6 nA/mm^2 in the case of dual wire-cylinder electrode (curve 1), with "limiting cylinder" and by 28%, from $J_{\max}$ = 10.5 nA/mm^2 to $J_{12.5mm}$ = 7.5 nA/mm^2 in the case of the dual wire – cylinder electrode.

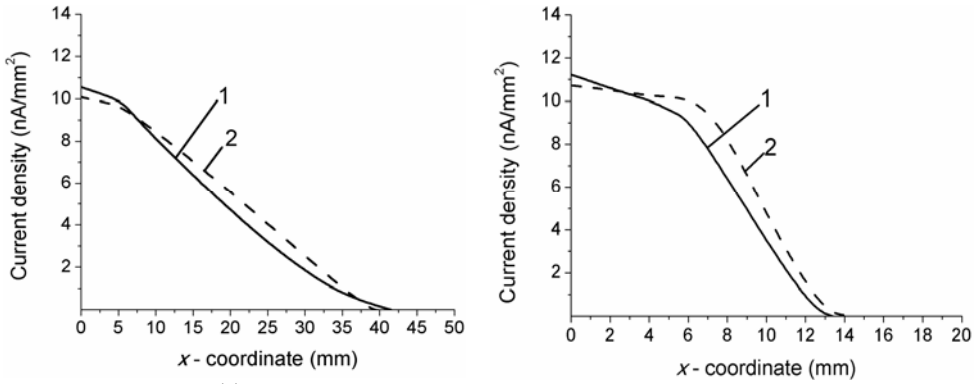

Fig. 10. Variations of the experimental (1) and computed (2) current densities with *x*-coordinate for the dual wire-cylinder electrode (a) and dual wire-cylinder with limiting cylindre (b) ($y = 0$, $a = 25$ mm, $V_0 = 24$ kV)

The use of the limiting cylinder reduces the surface of the plate electrode where the courant density (and the space charge density) takes important values. But this area does not modify significantly with the distance a between the ionizing wire and cylinder in the case of dual electrode (curves 2 and 3).

At $V_0 = 24$ kV, in the absence of the "limiting cylinder", the total electric current per unit of length measured at the surface of the plate-type electrode is 446.15 μA/m, which is by 35.1 % higher than the total current measured in the presence of the "limiting cylinder".

4. Validation of computed values

Figure 10 presents the variations with x – coordinate of the current densities, experimentally determined (curves 1) and calculated (curves 2). It may be seen that, in both cases, the experimental values are close to the calculated ones, but slightly lower. This may be due to the imperfections of fixing the dual electrode, the limiting cylinder besides ionizing wire and grounded plate. Also, these errors may be caused by the supplementary metallic elements used to sustain the limiting cylinder fixed on the dual electrode.

5. Conclusions

The model proposed in this paper enables the computation of ionic space charge density and the electric field repartition in the case of corona discharges produced by dual electrodes with "limiting cylinder".

The values of the computed current density are quite close to the experimental determined ones, validating the precision of the calculation model.

From a practical point of view, the use of the "limiting cylinder" leads to an increase of the electric field and space charge volume density during the charging process of filtration media. At the same time, it may block the electric charges produced by corona discharges from dissipating to other grounded equipments which may be near the charging installation.

Acknowledgements

This work has been supported by the Sectoral Operational Programme Human Resources Development 2007-2013 of the Romanian Ministry of Labour, Family and Social Protection through the Financial Agreement POSDRU/88/1.5/S/60203 and POSDRU/89/1.5/S/62557.

Fruitful discussions with Prof. A. Morega and Dr. A. Dobre regarding the use of Comsol Mutiphysics software are acknowledged with thanks.

R E F E R E N C E S

[1] *M. C. Plopeanu, P. V. Notingher, L. M. Dumitran, B. Tabti, A. Antoniu and L. Dascalescu*, "Surface Potential Decay Characterization of Non-woven Electret Filter Media", in IEEE Transactions on Dielectrics and Electrical Insulation, **vol. 18**, issue 5, 2011, pp. 1393 – 1400

[2] *N. S. Billington*, "Air filtration", in Journal of the Institution of Heating and Ventilation Engineers, **vol. 14**, 1947, pp. 46-95

[3] *J. Van Turnhout, W. J. Hoeneveld, J. W. C. Adamse and L. M. Van Rossen*, "Electret Filters for High – Efficiency and High-Flow Air Cleaning", in IEEE Transactions on Industry Applications, **vol. 17**, 1981, pp. 240-248

[4] *D.C. Walsh and J. I. T. Stenhouse*, "Parameters Affecting the Loading Behavior and Degradation of electrically active Filter Materials", in Journal of Aerosol Science and Technology, **vol. 29**, 1998, pp. 419 – 432

[5] *F.J. Romay, B. Y. H. Liu and S. J. Chae*, "Experimental study of electrostatic capture mechanisms in commercial electret filters", in Journal of Aerosol Science and Technology, **vol. 28**, 1998, pp. 224 – 234

[6] *D. L. Myers and B. D. Arnold,* "Electret Media for HVAC Filtration Applications", in International Nonwovens Journal, **vol. 12**, no. 4, 2003, pp. 43 - 53

[7] *W. J. Jasper, A. Mohan, J. Hinestroza and R.Barker*, "Degradation processes in corona-charged electret filter-media with exposure to ethyl benzene", in Journal of Engineered Fibers and Fabrics, **vol. 2**, 2007, pp. 1– 6

[8] *T. Butonoi, G. Gagiu, M. Bilici, A. Samuila, V. Neamtu, R. Morar, L. Dascalescu and A. Iuga*, "Electric and Electronic Equipment of a Research – Oriented Electrostatic Separator", 12th International Conference and Optimization of Electrical and Electronic Equipment, OPTIM 2010, pp. 639 – 645

[9] *E. C. Starr*, "High Voltage D.C. Point Discharges", in IEEE Transactions of the American Institute of Electrical Engineers, **vol. 60**, issue 6, 1941, pp. 356 – 362

[10] *D. Rafiroiu, R. Morar, P. Atten and L. Dascalescu*, "Premises for the Mathematical Modeling of the Combined Corona – Electrostatic Field of Roll-type Separators", in IEEE Transactions on Industry Applications, **vol. 36**, no. 5, 2000, pp. 1260 – 1266

[11] *L. M. Dumitran, L. V. Badicu, M. C. Plopeanu and L. Dascalescu*, "Efficiency of Dual Wire – Cylinder Electrodes Used in Electrostatic Separators", in Revue Roumain des Sciences Techniques**, vol. 55**, issue 2, 2010, pp. 171 – 180

[12] *J. A.Giacometti and O. N.Oliveira Jr.*, "Corona Charging of Polymers", in IEEE Transactions on Electrical Insulation, **vol. 27**, no. 5, Oct. 1992, pp. 924 – 943

[13] *P. Sattari*, FEM-FCT Based Dynamic Simulation of Trichel Pulse Corona Discharge in Point – Plane Configuration, PhD Thesis, University of Western Ontario, 2011

[14] *M. Darnon*, Les Procedes par Plasmas Impliques dans l'Integration des Materiaux SiOCH Poreux pour les Interconnexions en Microelectronique, PhD Thesis, University Grenoble I – Joseph Fourier, 2007

[15] *J. J. Lowke and R. Morrow*, "Theory of Electric Corona Including the Role of Plasma Chemistry", in Journal of Pure and Applied Chemistry, **vol. 66**, no. 6, 1994, pp. 1287 – 1294

[16] *D.V. Rafiroiu*, Analyse numérique des champs électriques à charges d'espace. Application à la conception assistée par ordinateur des séparateurs couronne-électrostatiques, PhD Thesis, Universitatea Tehnica din Cluj-Napoca and Université Joseph-Fourier de Grenoble, 1999

[17] *A. Caron and L. Dascalescu*, "Numerical Modeling of Combined Corona – Electrostatic Field", Journal of Electrostatics, **vol. 61**, 2004, pp. 43 – 55

[18] *L. M. Dumitran, P. Atten, P. V. Notingher and L. Dascalescu*, "2-D Corona Field Computation in Configurations with Ionising and Non-Ionizing Electrodes", in Journal of Electrostatics, **vol. 64**, issues 3 – 4, 2006, pp. 176 – 186

[19] *L. M. Dumitran, L. Dascalescu, P. Atten and P. V. Notingher*, "Computational and Experimental Study of Ionic Space Charge Generated by Combined Corona – Electrostatic Electrode System", in IEEE Transactions on Industry Applications, **vol. 42**, no. 2, 2006, pp. 378 – 384

[20] *D. Rafiroiu, I. Saurasan, R. Morar, P. Atten and L. Dascalescu*, "Corona Inception in Typical Electrode Configurations for Electrostatic Processes Applications", in IEEE Transactions on Industry Applications, **vol. 37**, no. 3, 2001, pp. 766 – 771

[21] *B.Khaddour*, Modélisation du champ electrique modifié par la charge d'espace injectée, PhD. Thesis, Institut National Polytehnique de Grenoble, 2006

[22] *P. Atten*, Etude mathématique du problème de champ électrique affecte par un flux permanent d'ions unipolaires et applications à la théorie de la sonde froide, PhD. Thesis, Université de Grenoble, 1969

[23] *L.M. Dumitran*, Collection des fines particules dans un dépoussiéreur électrostatique, PhD Thesis, Université Joseph Fourier – Grenoble 1 and Universitatea "Politehnica" din Bucuresti, 2001